Pure Appl. Chem., Vol. 77, No. 2, pp. 379–389, 2005.
DOI: 10.1351/pac200577020379
© 2005 IUPAC

Exploration of the deposition limits of microcrystalline silicon*

D. Mataras‡

Plasma Technology Laboratory, Department of Chemical Engineering, University of Patras, P.O. Box 1407, 26504 Patras, Greece

Abstract: The effect of various process parameters on the deposition rate of microcrystalline hydrogenated silicon is presented. The various pathways leading to high deposition rates involve the optimization of a combination of parameters, while maintaining the crystalline character of the film and avoiding the presence of particles. The deposition rate increases in conditions that enhance and at the same time "cool down" the electron population. Such conditions are: moderately higher frequencies, higher pressures, and the presence of larger molecules (like disilane) even in small quantities. There is an optimum pressure, determined by primary dissociation, for a certain silane fraction. In addition, silane fraction and power density must also increase up to the limit of transition to amorphous growth and before attachment becomes too important. In all of these cases, there is a need for optimizing the distance of the deposition substrate to the source of radical generation, especially at higher pressures, to further increase the already important contribution of higher silicon radicals. It is shown that similar deposition rates can be obtained via radical fluxes with very different compositions. In every case, there is a need for sufficient H atom fluxes to ensure crystalline growth.

Keywords: microcrystalline silicon; silane; plasma-enhanced CVD.

INTRODUCTION

Amorphous silicon (a-Si:H) and microcrystalline silicon (μc-Si:H) thin films are similar in many aspects. They were probably not even distinguished in the early years of enthusiasm, although μc-Si:H has been early recognized among the variety of structures resulting at certain deposition conditions [1]. However, it is the dissimilarities between the two materials that have provoked new interest in thin film silicon applications [2–6], and thereof in optimizing plasma-enhanced chemical vapor deposition (PECVD) from silicon-containing gases for producing μc-Si:H [5–8], as well as in prospecting interesting material properties around the a-Si:H/μc-Si:H growth transition [6,9–13]. The use of μc-Si:H as the absorber layer in a-Si:H/μc-Si:H tandem solar cells especially promise significantly higher and stable efficiencies than what is achieved today with conventional a-Si:H technology [14], current achievements reaching initial efficiencies of 14.5 % [15].

In any case, the use of the same process technology for both materials is an additional advantage because one can use almost the same equipment and know-how that are already used in production. Still, the two processes are only partially alike, mostly because of the high hydrogen dilution of the silicon precursor gas and the quite different operation regimes used for depositing μc-Si:H. In fact, highly diluted silane discharges are in many ways different from the thoroughly studied pure silane or pure hydrogen discharges, and, thus, the accumulated extensive related literature on the deposition of a-Si:H is

*Paper based on a presentation at the 16th International Symposium on Plasma Chemistry (ISPC-16), Taormina, Italy, 22–27 June 2003. Other presentations are published in this issue, pp. 345–495.

‡E-mail: dim@plasmatech.gr

not particularly enlightening [16]. Nevertheless, the need for studying SiH_4/H_2 discharges does not rise from pure scientific interest only; the increase of the film growth rate is a critical technical issue that needs to be solved rapidly while being attentive to the associated quality issues. In reality, there is a need for at least a one order of magnitude increase of the deposition rate, while maintaining acceptable quality, in order to be able to reach viable production conditions. This is due to the need for thicker i-layers compared to a-Si:H, to compensate for the lower absorption of μc-Si:H in the visible region.

In this direction, many new, even radical ideas have been proposed, including hot-wire CVD [17], inductive and microwave plasmas [18,19], expanding thermal plasma, and hollow cathode [20,21]. Apart from the promising aspects as well as the inevitable limitations of each of these methods, compatibility with existing equipment, accumulated experience and large area deposition requirements, features already offered by PECVD from SiH_4/H_2 mixtures, make the optimization or the reinvention of the latter method the preferable choice. In that sense, much effort has been spent in the last few years in exploring systematically various more or less conventional operating regimes [2–14,22–24]. Among these, the use of higher excitation frequencies and the so-called, high-pressure depletion regime seem to be the most popular techniques in current literature, both with encouraging results, whereas new ideas also emerge [25]. However, concerning the evaluation of each solution, although different material characterization methods maybe useful, the ultimate test that could decide for these new layers, is to incorporate them in actual solar cells. Evidently, there is still a long way to go for testing and fully exploring the potential of all the proposed solutions in optimized solar cells.

The purpose of this paper is to report on the continuing efforts toward the limits of the PECVD from highly diluted SiH_4 in H_2, by isolating as much as possible the effect of the principal parameters that govern the process and can have an effect on the growth rate and the structure of thin silicon films. This discussion is focused on the process point of view without going into an in-depth discussion of the structural or the optoelectronic properties of the range of materials produced.

METHODOLOGY

Despite the large amount of work on the subject, there is still a series of open questions concerning methodological and experimental details, obscuring clear conclusions on the mechanism and the limits of μc-Si:H growth. As an example of this, one could mention here two common issues: the well-known particle formation problem and the problem of controlled/reproducible conditions.

Besides the effects of dust particles on the deposited film structure and properties that are not discussed here, one thing is certain: a discharge containing dust particles is completely different in both properties and film growth from a particle-free discharge [26,27]. However, although there are many "signs" of the presence of particles, including various sensitive plasma diagnostics, the presence of particles during the reported deposition experiments is hardly ever mentioned in the literature. One of the serious consequences of this is the impossibility to evaluate the validity of data and to reproduce the experiments in other systems, taking also into account that the formation of particles depends very much on different characteristics of the chamber (shields, edges, heating, etc.) as well as on the route followed toward adjusting the specific operating conditions.

On the other hand, reproducibility does not suffer only from the presence of dust particles, but also from the lack of control of crucial parameters like the real power going into the discharge and the impedance of the cell, which among other things, is also sensitive to the deposition history of the chamber. It is wrongly believed that if one maintains a constant radio frequency (rf) generator output level, the power going into the discharge will also be constant. The truth is that for the same rf generator output, the power consumption does not depend only on the system, but it is also greatly influenced from other common discharge parameters like gas composition, pressure, and geometry, not to mention the discharge excitation frequency [22,24]. Moreover, this is only a part of the story since it is not only a question of the total power, but also of the way this power is spent in various elementary subprocesses.

The two factors just mentioned are merely examples showing the diversity of aspects that need to be examined when exploring a process of such complexity. In general, the limits of μc-Si:H growth, for a certain deposition temperature, depend on the rate of arrival of silicon precursors vs. the rate of their accommodation in the growing film network, and this is thought to be mediated by a high flux of hydrogen atoms [14,16,28–30]. The flux of silicon precursors will in turn depend on their space-dependent rate of generation as well as on their gas-phase reactivity vs. transport to the deposition surface. However, not all silicon precursors are equal either in generation or in gas and surface reactivity. Finally, the generation of these precursors depends on the magnitude and the spatial distribution of an effective electron density as well as on the concentration of other charged and neutral species. All of these microscopic parameters and many more are naturally related to each other as parts of the same complex collective system. It is evident, from this nonexhaustive description, that if one is set to explore the limits of such a system, there are two prerequisites: (a) accurate experimental measurements, isolating as much as possible the effect of each parameter from all of the others, and (b) a model of the process as close to reality as possible, to be able to analyze and extrapolate results in such a way that transferability and scale-up of recipes is made possible.

In the following paragraphs, we will present experimental results concerning as much as possible the net effect of the main process parameters, we will further analyze the results using specially developed models, and finally we will compare both theoretical and experimental results with the current literature. All of the results presented concern deposition experiments carried out in capacitively coupled rf discharge chambers that are completely characterized from the electrical point of view in such a way that the power actually consumed in the discharge is accurately known through voltage and current waveform measurements [31]. Moreover, to the best sensitivity of our laser-scattering diagnostics, the discharges operate in particle-free conditions, unless specifically stated otherwise.

RESULTS AND DISCUSSION

In the following paragraphs, we intend to present the effects of some of the main process parameters on the deposition rate and in general the efficiency of the discharge. The reader should keep in mind that in most of the cases, the experiments presented are not designed to achieve the highest possible deposition rates, but to bring up the correlation instead.

Frequency

The increase of frequency above the usual 13.56 MHz has been proposed to be beneficial for the deposition rate, as well as for the crystallinity of the films [32–35]. However, these observations were attributed to a variety of somewhat controversial reasons ranging from the enhancement of the electron impact dissociation of SiH_4 to a higher surface reactivity owing to an increase of the ion flux. On the other hand, the reduction of the ion bombardment energy or the higher atomic hydrogen flux toward the growing film surface, were proposed for explaining the beneficial effect on the crystallinity of the film.

We believe that the only way to evaluate the effects and exploit the possible benefits is to vary the frequency while keeping a constant power density in the discharge, otherwise the inevitable decrease of the necessary sustaining voltage with increasing frequency leads to false impressions since the power going into the discharge increases with frequency [22,24,37]. VHF is associated with very high power losses in the feed lines, as well as with deposition non-uniformities owing to standing and evanescent waves on large-area electrodes [36].

Figure 1 presents the effect of frequency, varied in a range where large-area uniformity is still not a problem, on both the measured deposition rate [22] and the calculated electron impact dissociation rate of silane [16]. As frequency increases, the constant power dissipation induces a drop of the electric field, an increase of the electron density and an enhancement of the power consumed by electrons.

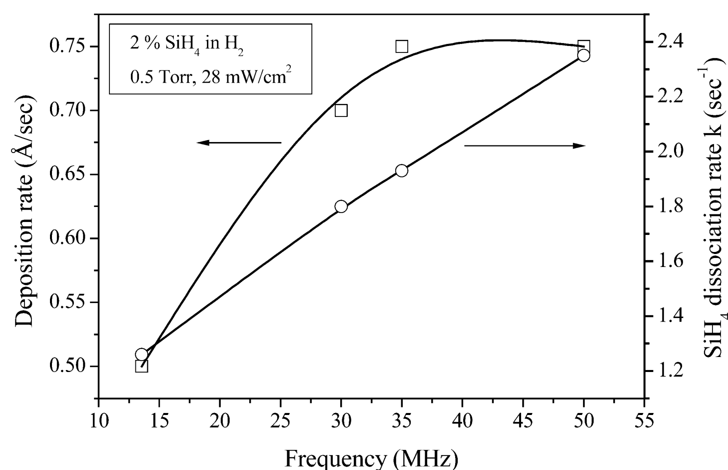

Fig. 1 Variation of the deposition rate (left axis) and the apparent dissociation rate *k* (right axis) with frequency at constant rf power, pressure, and silane %.

These changes lead to a decrease of the rate of the high-energy electron-molecule collision processes, thus favoring silane and hydrogen dissociation while reducing the chance for particle formation. The increase of the hydrogen flux toward the surfaces is the main reason favoring the growth of µc-Si:H thin films. However, as seen in Fig. 1, the increase of the deposition rate is not solely related to the increase of SiH_4 dissociation induced by the increase of the effective electron density. It is also a question of transport vs. reactivity of the precursors. Highly sticking and highly reactive radicals, like SiH_2, may have the chance to contribute significantly when their diffusion length is smaller than the interelectrode gap at the specific conditions.

Therefore, as seen in Fig. 2, the growth rate is very sensitive on the spatial distribution of the source of these radicals. The displacement of the maximum rate of radicals' production toward the rf electrode with increasing frequency (smaller sheaths), leads to a weakening of the dependence of the deposition rate on SiH_4 dissociation.

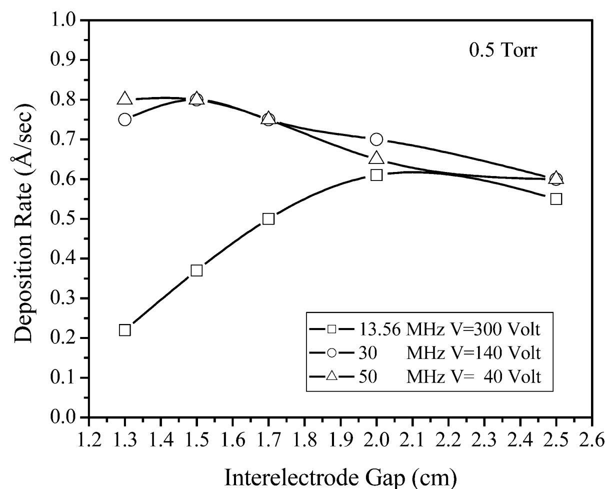

Fig. 2 Deposition rate as a function of the distance between the two electrodes for three different excitation frequencies at constant rf power (28 mW/cm^2) and dilution (98 % H_2).

Dilution and pressure

The increase of the silane content is another measure for enhancing the deposition rate. However, this is limited by the transition to amorphous growth and/or the appearance of dust particles because of the increasing importance of attachment reactions.

In Fig. 3, we present the effect of silane fraction at two different pressures, keeping constant power dissipation at each one. The deposition rate is doubled for the lower pressure, while it is four times higher for the higher pressure when going from 2 to 6 %. Silane consumption is increasing almost as the increase of its percentage in both cases. These clear conclusions are only possible because we know the power is constant, otherwise the increase of percentage would also lead in a serious variation of the power actually consumed in the discharge.

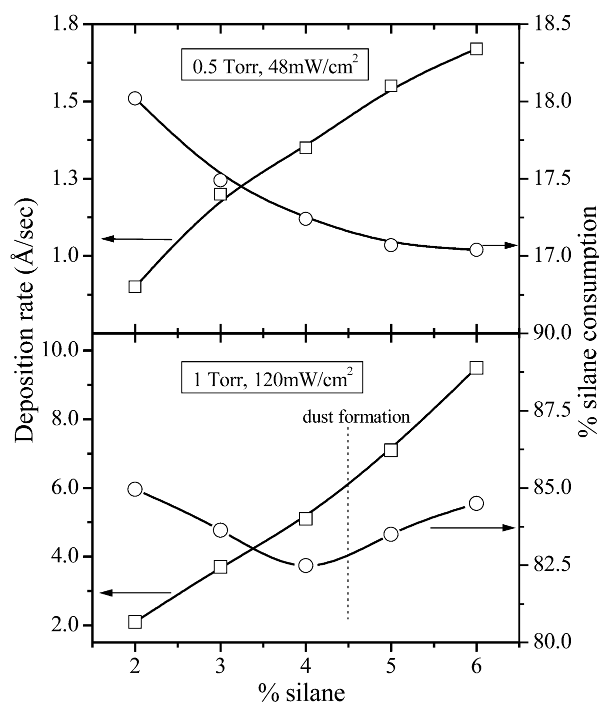

Fig. 3 Deposition rate (left axis) and % silane consumption (right axis) as a function of the percentage of silane in hydrogen at two different pressures (0.5 upper and 1 torr lower).

These results can be further discussed in terms of reactivity vs. transport of the main radicals, by means of numerical modeling based on experimental measurements of radical generation in space, silane consumption, and deposition rate [16].

As shown in Fig. 4, for the case of 0.5 torr, the increase in silane content leads to a relative enhancement of the SiH_x/H flux ratio, and this is more pronounced for the much less reactive Si_xH_{2x+1} than for the highly reactive Si_xH_{2x} radicals. Under these conditions, Si_xH_{2x} radicals can contribute more to the film growth owing to their higher surface incorporation probability [23], still there is a drop of the SiH_2 radical flux relative to SiH_3. Furthermore, higher silane fractions directly favor the hydrogen insertion reaction leading to a reduction of H atom transport to the surface. The transition from microcrystalline to amorphous silicon deposition, which is usually observed when the SiH_4 fraction increases, is thus mostly related to the decrease of H atoms flux relative to all other species.

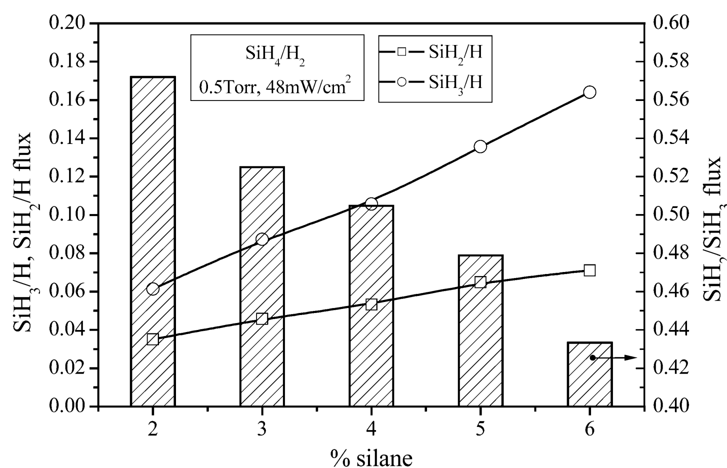

Fig. 4 SiH_3/H_2 and SiH_2/H_2 (left axis) as well as SiH_2/SiH_3 (bars, right axis) species flux ratios to the growing film surface as a function of silane percentage at constant rf power and pressure.

On the other hand, the increase of the total pressure has analogous transport consequences with the increase of % SiH_4 while having somewhat similar effects on primary dissociation with the increase of frequency. As in the case of frequency, the electron density increases and analogous high deposition rates can be achieved by increasing power, however, attachment is facilitated instead of being suppressed. Silane consumption increases although the electron impact dissociation constant decreases [38]. The effective advantages of increasing the pressure are best shown in Fig. 5, which summarizes the effect of pressure and the various ways leading to an increase of the deposition rate with primary dissociation. It results from this figure that 26 % of the silicon atoms initially produced through electron impact dissociation are incorporated in the film at 1 torr, whereas this figure falls to only 12 % for the pressure of 0.5 torr. In any case, the conclusion drawn from this figure is that there is no single parameter that could be adjusted to obtain the desired deposition rate. Instead, there is more than one combination leading to a variety of materials that can only be distinguished through systematic characterization and testing in actual solar cells.

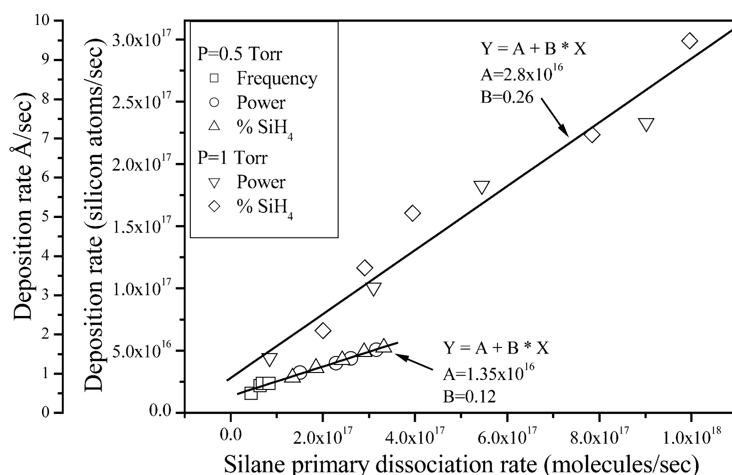

Fig. 5 Deposition rate in Å/s and in Si atoms flux/s arriving on the total heated deposition electrode area vs. the electron impact dissociation rate of silane for two different pressures. Different sets of data recorded while varying frequency, % SiH_4 and rf power are included.

High-pressure regime

Substantially higher pressures than those examined so far have been suggested to lead to higher deposition rates while maintaining a good film quality [6–8]. The regime was called high-pressure depletion because the saturation of the deposition rate with increasing pressure was attributed to a depletion of silane that would suppress somewhat the reaction of H atom insertion to silane [39,40]. Thus, H atoms would be available for the growth.

Thus, in order to examine the effect of total pressure we conducted experiments in the range of 1 to 10 torr while maintaining constant power and at the same time constant silane partial pressure. The result of 53 experiments is shown in Fig. 6. There is a clear maximum for a pressure of 2.5 torr while the effect of interelectrode space variation depends also very much on pressure depicting very well various areas of transport restriction and contribution of Si_xH_{2x} radicals. But what is more spectacular is that the observed variation of the deposition rate with pressure is repeated exactly in the variation of the total emission intensity from two excited species with different appearance thresholds as shown in Fig. 7. Silane consumption never exceeds 50 % in the given conditions, and the films obtained over the entire range are highly crystalline. It seems that at the specific conditions the deposition rate is directly determined by the primary dissociation of silane through electron impact.

We have repeated these experiments and obtained similar results for another frequency and another dilution, and we obtained similar results showing a single maximum deposition pressure, the position of which depends only on the silane content.

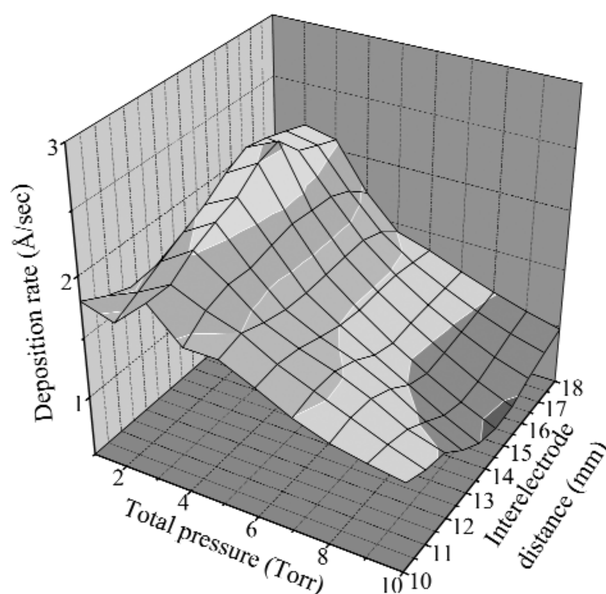

Fig. 6 Experimental measurements of the deposition rate as a function of pressure and interelectrode distance at constant silane content (25 mtorr) and constant rf power (72 mW/cm^2) for a 27.12 MHz discharge.

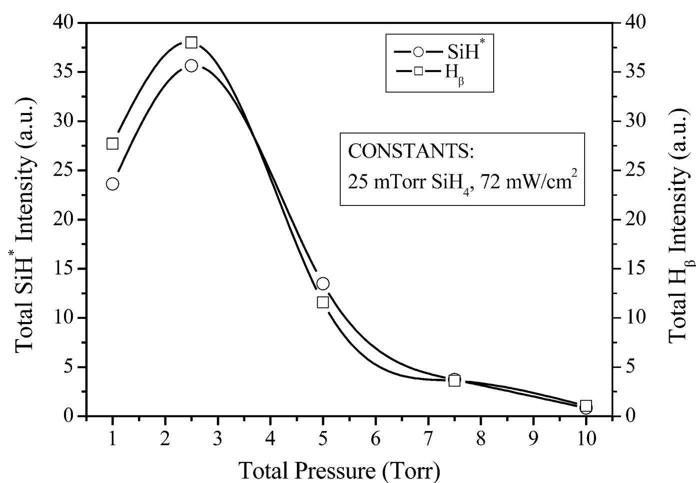

Fig. 7 Total emission intensities of $SiH^*(A^2\Delta)$ and H_β as a function of total pressure at constant silane content (25 mtorr) and constant rf power (72 mW/cm^2). The total intensities are obtained by integrating spatial emission profiles obtained with a resolution better than 1 mm in the interelectrode space.

Gas mixtures

Alternative silicon precursor and dilution gases have been proposed in the past as another way for increasing the deposition rate, but this is still a much less popular solution than the ones previously mentioned for several practical reasons [30,41,42]. Also, in this case, one is after higher electron densities and lower electron energies that would favor silane dissociation at a gas density that would not favor attachment. We have recently investigated deposition of microcrystalline silicon thin films from $SiH_4/Si_2H_6/H_2$ mixtures. Especially, a small addition of Si_2H_6 in SiH_4/H_2 discharges was found to increase the power consumption significantly and have a catalytic effect in silane dissociation. As shown in Fig. 8, the increase of the Si_2H_6 fraction from 0 to 0.6 % under constant power dissipation results in a spectacular increase of the deposition rate by more than six times. This increase has been proved that is not induced by the increase of silicon atom density in the reactor and has been attributed to the enhancement of silane dissociation caused by an increase of the electron density [25].

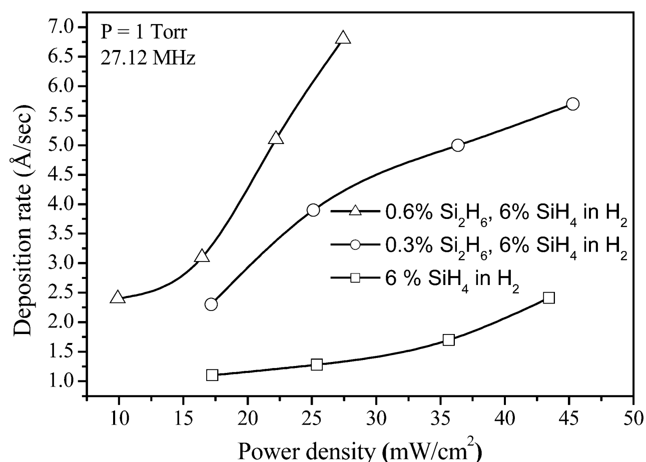

Fig. 8 Deposition rate as a function of power in three different mixtures containing 6 % silane in hydrogen. 0.3 and 0.6 % disilane was added, respectively, in two of the mixtures.

The question that arises is, how one can compare these conditions to the ones previously presented. Figure 9 is a perfect example of the wide variety of situations leading to films with similar structure and optoelectronic properties. The figure is based on the results of a numerical simulation that is in close agreement with measurable experimental quantities like the deposition rate and the effluent composition [16]. These four films are deposited under quite different conditions, by a different flux of precursors leading to different growth-dominant species in each case. What is common between them is that there is in every case an important contribution of species with two or more silicon atoms and a high H atom flux to the surface, assuring for the crystalline character of the growing film. There is still a ways to go before identifying if one of them or more represent an advance the right direction.

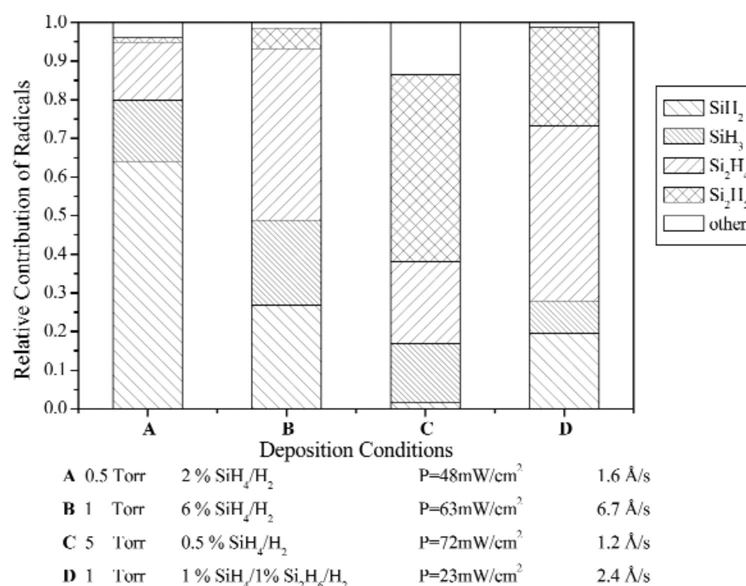

Fig. 9 Relative contribution of radicals in the deposition rate at four distinct deposition conditions.

SUMMARY

The effect of various parameters on the deposition rate of μc-Si:H has been presented. The conclusion drawn is that there are many different ways that can lead to high deposition rates and all of them involve the optimization of a combination of parameters, taking into account that the crystalline character of the film must be maintained. The right way is definitely the one that would lead to the best device efficiency when tested in actual solar cells, taking into account also other parameters of economic nature.

The results presented were chosen for justifying the need for controlled and repeatable deposition conditions, in order to draw clear conclusions on the specific effect of each one of the main deposition parameters.

In general, the deposition rate is increased through conditions that increase and at the same time "cool down" the electron population. Thus, the dissociation of both silane and hydrogen is increased, leading to higher fluxes of radicals and atomic hydrogen to the surface. Such conditions are: moderately higher frequencies, higher pressures, and the presence of larger molecules (like disilane) even in small quantities. Among them, frequency has a definitive advantage of not favoring attachment at the same time and thus is a measure that must be taken anyhow. Moreover, there is an optimum pressure for a certain silane fraction that seems to be determined by the primary dissociation of silane. In addition to these, one can also increase the silane fraction and the power density up to the limit of transition to amorphous growth and before attachment becomes too important. In all of these cases there is a need

for reoptimizing the distance of the deposition substrate to the source of radical generation, especially at higher pressures, to further increase the already important contribution of higher silicon radicals.

It has been shown that similar deposition rates can be obtained via radical fluxes with very different compositions. In every case, there is a need for sufficient H atom fluxes to ensure crystalline growth.

ACKNOWLEDGMENT

This work was performed in the framework of the EU-funded DOIT (ENK6-CT-2000-00321) research project.

REFERENCES

1. S. Veprek and V. Marecek. *Solid State Electron.* **11**, 683 (1968).
2. J. Meyer, R. Flückiger, H. Keppner, A. Shah. *Appl. Phys. Lett.* **65**, 860 (1994).
3. K. Saito, M. Sano, K. Matsuda, T. Kondo, T. Nishimoto, K. Qgawa, I. Kajita. *Proceedings of the 2nd World Conference and Exhibition on Photovoltaic Solar Energy Conversion*, J. Schmid, H. A. Ossenbrink, P. Helm, H. Ehmann, E. D. Dunlop (Eds.), pp. 351–354 (1998).
4. K. Yamamoto, M. Yoshimi, Y. Tawada, Y. Okamoto, A. Nakajima. *J. Non-Cryst. Solids* **226–269**, 1082 (2000).
5. O. Vetterl, F. Finger, R. Carius, P. Hapke, L. Houben, O. Kluth, A. Lambertz, A. Mück, B. Rech, H. Wagner. *Sol. Energy Mater. Sol. Cells* **62**, 97 (2000).
6. T. Roschek, T. Repmann, J. Müller, B. Rech, H. Wagner. *J. Vac. Sci. Technol., A* **20**, 492 (2002).
7. B. Rech, O. Kluth, T. Repmann, T. Roschek, J. Springer, J. Müller, F. Finger, H. Stiebig, H. Wagner. *Sol. Energy Mater. Sol. Cells* **74**, 439 (2002).
8. B. Rech, T. Roschek, T. Repmann, J. Müller, R. Schmitz, W. Appenzeller. *Thin Solid Films* **427**, 157 (2003).
9. Y. Lubianiker, Y. Tan, J. D. Cohen, G. Ganguly. *J. Non-Cryst. Solids* **266–269**, 450 (2000).
10. J. Y. Ahn, K. H. Jun, K. S. Lim, M. Konagai. *Appl. Phys. Lett.* **82**, 1718 (2003).
11. S. Guha, J. Yang, A. Banerjee, B. Yan, K. Lord. *Sol. Energy Mater. Sol. Cells* **78**, 329 (2003).
12. R. W. Collins and A. S. Ferlauto. *Curr. Opin. Solid State Mater. Sci.* **6**, 425 (2002).
13. P. Roca i Cabarrocas. *Curr. Opin. Solid State Mater. Sci.* **6**, 439 (2002).
14. A. V. Shah, J. Meier, E. Vallat-Sauvain, N. Wyrsch, U. Kroll, C. Droz, U. Graf. *Sol. Energy Mater. Sol. Cells* **78**, 469 (2003).
15. K. Yamamoto, A. Nakajima, M. Yoshimi, T. Sawada, S. Fukuda, K. Hayashi, T. Suezaki, M. Ichikawa, Y. Koi, M. Goto, H. Takata, Y. Tawada. *Proceedings of the 29th IEEE Photovoltaic Specialist Conference*, pp. 1110–1113, New Orleans (2002).
16. E. Amanatides, S. Stamou, D. Mataras. *J. Appl. Phys.* **90**, 5786 (2001).
17. E. Iwaniczko, Y. Xu, R. E. I. Schropp, A. H. Mahan. *Thin Solid Films* **430**, 212 (2003).
18. N. Kosku, F. Kurisu, M. Takegoshi, H. Takahashi, S. Miyazaki. *Thin Solid Films* **435**, 39 (2003).
19. H. Shirai, Y. Sakuma, K. Yoshino, H. Ueyama. *Sol. Energy Mater. Sol. Cells* **66**, 137 (2001).
20. C. Smit, B. A. Korevaar, A. M. H. N. Petit, R. A. C. M. M. van Swaaij, W. M. M. Kessels, M. C. M. van de Sanden. *Proceedings of the 29th IEEE Photovoltaic Specialist Conference*, pp. 1170–1173, New Orleans (2002).
21. T. Tabuchi, M. Takashiri, H. Mizukami. *Surf. Coat. Technol.* **173**, 243 (2003).
22. E. Amanatides, D. Mataras, D. E. Rapakoulias. *J. Appl. Phys*. **90**, 5799 (2001).
23. E. Amanatides, D. Mataras, D. E. Rapakoulias, *Thin Solid Films* **383**, 15 (2001).
24. E. Amanatides, D. Mataras, D. E. Rapakoulias. *J. Vac. Sci. Technol., A* **20**, 68 (2002).
25. A. Hammad, E. Amanatides, D. Mataras, D. E. Rapakoulias. *Thin Solid Films* **451–452**, 255 (2004).

26. Ch. Hollenstein. *Plasma Phys. Control. Fusion* **42**, R93 (2000).
27. A. Gallagher, G. Bano, K. Rozsa. *Sol. Energy Mater. Sol. Cells* **78**, 27 (2003).
28. A. Matsuda, M. Takai, T. Nishimoto, M. Kondo. *Sol. Energy Mater. Sol. Cells* **78**, 3 (2003).
29. S. Sriraman, S. Agarwal, E. Aydil, D. Maroudas. *Nature* **418**, 62 (2002).
30. M. Jana, D. Das, A. K. Barua. *J. Appl. Phys*. **91**, 5442 (2002).
31. N. Spiliopoulos, D. Mataras, D. E. Rapakoulias. *J. Vac. Sci. Technol., A* **14**, 2757 (1996).
32. H. Curtins, N. Wyrsch, A. Shah. *Electron. Lett.* **23**, 228 (1987).
33. F. Finger, P. Hapke, M. Luysberg, R. Carius, H. Wagner. *Appl. Phys. Lett.* **65**, 2588 (1994).
34. A. A. Howling, J.-L. Dorier, Ch. Hollenstein, U. Kroll, F. Finger. *J. Vac. Sci. Technol., A* **10**, 1080 (1992).
35. M. Heintze, R. Zedlitz, G. H. Bauer. *J. Phys. D: Appl. Phys.* **26**, 1781 (1993).
36. J. Rüdiger, H. Brechtel, A. Kottwitz, J. Kuske, U. Stefan. *Thin Solid Films* **427**, 16 (2003).
37. E. Amanatides and D. Mataras. *J. Appl. Phys.* **89**, 1556 (2001).
38. E. Amanatides, D. E. Rapakoulias, D. Mataras. *J. Phys. IV*, **11**, Pr3-715 (2001).
39. L. Guo, M. Kondo, M. Fukawa, K. Saitoh, A. Matsuda. *Jpn. J. Appl. Phys.* **37**, L1116 (1998).
40. M. Kondo, M. Fukawa, L. Guo, A. Matsuda. *J. Non-Cryst. Solids* **266–269**, 84 (2000).
41. W. Futako, T. Takagi, T. Nishimoto, M. Kondo, I. Shimizu, A. Matsuda. *Jpn. J. Appl. Phys.* **38**, 4535 (1999).
42. T. Takagi, R. Hayashi, G. Ganguly, M. Kondo, A. Matsuda. *Thin Solid Films* **345**, 75 (1999).